

An Algorithmic Scheme for Construction and Investigation of Parkinson's Disease Model *

I. Gurevich¹, E. Kozina², A. Myagkov¹, H. Niemann³, M. Ugrumov² and V. Yashina¹

¹ Dorodnicyn Computing Centre of the Russian Academy of Sciences
Vavilov st. 40, 119333 Moscow, Russian Federation

² Koltzov Institute of Developmental Biology of the Russian Academy of Sciences
Vavilov st. 26, 119334 Moscow, Russian Federation

³ Friedrich-Alexander-University of Erlangen-Nurnberg
Martensstr. 3, Erlangen, 91058, Germany

Abstract. This work continues the development of mathematical tools and information technology elements for automated extraction and characterization of objects in striatum section images. The latter are used to construct a Parkinson disease model at a preclinical stage. Previously an automatic segmentation method for extracting of objects from striatum section image was developed. Now it is enhanced and extended to a form of an algorithmic scheme. It allows reducing brain section images to a form appropriate for recognition. Experimental applications of the developed technique have confirmed its high efficiency and suitability for automated processing and analysis of brain section images (a 200 times increase in productivity and a 10 times decrease in the amount of animals and expendables).

1 Introduction

This work is aimed at the development of mathematical tools and information technology elements for automated extraction and characterization of objects in striatum section images. The latter are used to construct a Parkinson disease (PD) model at a preclinical stage. The developed technique can be used to quantitatively estimate (a) the degeneration of dopaminergic (DA-ergic) axons in the striatum after specific DA-ergic neurotoxin administration; and (b) the functional condition of DA-ergic axons remaining after neurotoxin administration. For this task we adapted the standard algorithmic scheme developed previously for automated morphological image analysis of lymphoid cell nuclei of diseased hemoblasts [3, 4].

* This work was partially supported by the Russian Foundation for Basic Research Grant No. 09-07-13595, by the Program of Fundamental Research of the Presidium of the Russian Academy of Sciences (2010) and by the program "Participant of Young Scientific-Innovate Tender" ("U.M.N.I.K.") of the Foundation for Assistance to Small Innovative Enterprises (state contract Nos. 6956/9009, 6957/9010).

The study and modeling of PD [1] are an extremely topical problem in modern medicine. It is crucially important to detect the disease as early as possible and to automate its detection as much as possible. Thus, it is important to provide physicians and medical researchers with an automated computer system for early disease diagnostics at a preclinical stage. The creation and investigation of PD models is also important for the study of brain compensatory mechanisms with the aim of controlling them in the future.

The development of PD models requires a screening analysis of motor behavior regulation and dopamine (DA) metabolism in the nigrostriatal system with the use of various schemes for neurotoxin administration [7, 5]. DA-ergic neurons, which project axons to the striatum, are a key element in the regulation of motor behavior. Progressive degeneration of these neurons leads to the development of PD.

Morphological research underlying the construction of preclinical stage PD models is associated with the processing and analysis of a great amount of experimental data, such as images of serial brain sections in experimental animals. The study of each image includes the detection and calculation of quantitative and qualitative features for hundreds of neurons and thousands of their axons. Consequently, to construct and study adequate preclinical stage PD models efficiently, it is necessary to automate the processing and estimating of experimental data. In turn, this requires the development and study of suitable mathematical techniques and their implementation in the form of efficient algorithmic schemes and software systems.

Automated medical image-mining is based on the joint use of image processing techniques and the mathematical theory of image analysis and pattern recognition. The designed technique is represented as a specialized algorithmic scheme consisting of the following principal stages, which implement automated extraction of information from images: (1) preprocessing (image quality enhancement, elimination of irrelevant details and artifacts, statistical and logical filtering); (2) image analysis (detection of objects, extraction of their edges; segmentation; the choice and estimation of features describing the structure and content of images, etc.); (3) construction of object representations; (4) classification of objects presented in images.

In Section 2, we describe the initial data and the characteristics of a PD model. The method developed for the automated extraction and analysis of terminals of DA-ergic axons presented in striatum section images is briefly outlined in Section 3. An analysis of the method is given in Section 4. The steps in the algorithmic scheme and the results of its application to the initial data are described in detail in Section 5. The conclusions and the directions of further research are given in Section 6.

2 Initial Data and PD Model

The initial data were digital images of immunostained sections of various brain areas. DA-ergic neurons were labeled in serial sections (with a thickness of $20\mu m$) of the substantia nigra and their fibers (axons) were labeled in striatum sections with a thickness of $12\mu m$). The initial image resolution is $0.0117\mu m^2/pxel^2$.

Terminals are small rounded objects with an area varying from 0.6 to $3\mu\text{m}^2$. Terminals can have an oval, round, prolate or irregular shape. In the presented gray-scale images, the brightness of terminals is lower than the background brightness.

The PD model represents the differences between experimental and control groups. The former is a group of animals injected with a toxin, while the latter is a group of animals not affected by the toxin. Typical initial images for the control and experimental groups are presented in Figs. 1 and 2, respectively.

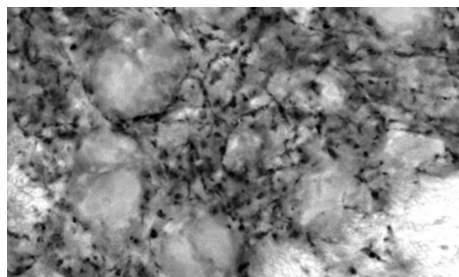


Fig. 1. Control initial image — a striatum section image of an animal not affected by the toxin.

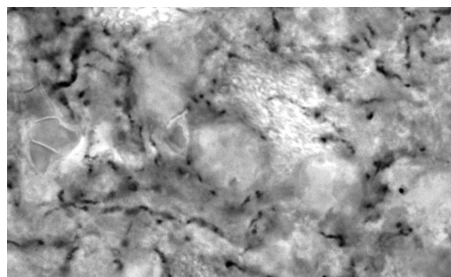


Fig. 2. Experimental initial image — a striatum section image of an animal injected with a toxin.

A major characteristic of the PD model is the number of DA-ergic axons innervating the striatum in the case of using various schemes for neurotoxin administration (dose, the number of injections, intervals between injections). The extent of degeneration is defined as the difference between the number of terminals of DA-ergic axons in the control and experimental groups. DA-ergic neurons and axons remaining after neurotoxin administration are supposed to demonstrate increased functional activity in order to compensate for the DA deficiency. An indicator of the increased functional activity of neurons and their fibers can be an increase in their sizes. An increase in the concentration of tyrosinehydroxylase (key enzyme in DA synthesis) is supposed to be another specific indicator of the functional activity of DA-ergic axons and neurons.

The data were presented by the Koltzov Institute of Developmental Biology of the Russian Academy of Sciences, Moscow, RF.

3 The Algorithmic Scheme

The authors have proposed new original methods for reducing medical images to a form suitable for recognition [3, 4]. The methods were used as a basis for developing standard algorithmic schemes for automated images.

The mathematical methods and algorithmic schemes developed were designed for (a) automated quantitative estimation of the degree of degeneration of DA-ergic axons (terminals) in the striatum as based on the difference between the numbers of terminals in the experimental and control groups; and for (b) automated estimation of the functional condition of distal segments of DA-ergic axons (terminals) in the striatum.

The developed algorithmic scheme consists of the following stages:

1. preprocessing:
 - (a) opening by reconstruction;
 - (b) the bot-hat transformation by dual reconstruction;
 - (c) closing by dual reconstruction;
 - (d) h-dome elimination transformation;
2. image analysis:
 - (a) object and background markers extraction;
 - (b) morphological gradient image modification;
 - (c) watershed segmentation;
3. construction of object representations:
 - (a) construction of feature descriptions (25 morphometric, densitometric, and textural features are used);
 - (b) feature selection;
4. classification:
 - (a) objects clustering;
 - (b) results interpretation.

The preprocessing and image analysis stages of the scheme are based on the following mathematical morphology operations: opening [6, 2], grayscale reconstruction [9], closing [6, 2], the bot-hat transformation [6, 2], morphological gradient [6, 2], and the watershed transformation [8]. The application of these steps to initial images enables one to smooth heterogeneous complex background, select small objects in images depending on given sizes and gray values, eliminate out-of-focus objects, and separate close objects.

A set of informative features is selected at the third stage of the algorithmic scheme. Interpretation of these features by PD experts can reveal some new patterns in the PD development.

At the fourth stage, the objects are clustered into several groups. The characteristics of the clusters are also offered to PD experts for detailed analysis.

4 Accuracy Estimation

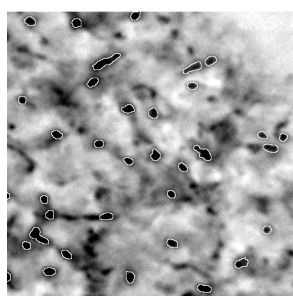
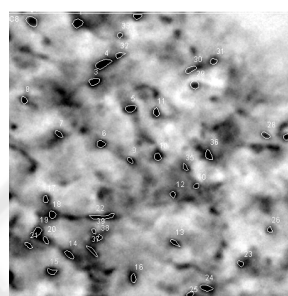
The accuracy of the results was evaluated by testing the hypothesis of feature probability distributions equality. Table 1 presents the feature statistics for manual and automated object extraction and the results of the two-sample Kolmogorov-Smirnov test. Inspection of the table suggests that the accuracy of the scheme is comparable with that of manual features estimation. In addition, the accuracy of terminals selection was estimated by counting the objects correctly found by PD experts. It turned out that 93% of the terminals were selected correctly.

The initial image with white marked object boundaries extracted by applying the proposed scheme is presented in Fig. 3. Figure 4 depicts the manually extracted objects for the same image.

According to PD experts, the proposed technique as applied to automated processing and analysis of brain sections provides a 200 times increase in productivity and a 10 times decrease in the amount of experimental animals and expendables.

Table 1. Comparison of manual and automated object extraction.

Statistics	Object extraction method	Area (μm^2)		Mean intensity		Number of Terminals	
		Experiment	Control	Experiment	Control	Experiment	Control
Mean	Automated	1.37	1.30	96.23	82.93	15.2	36.4
	Manual	1.56	1.52	95.79	83.60	13.6	34.6
Standard deviation	Automated	0.69	0.52	9.93	10.77	3.1	3.8
	Manual	0.57	0.70	10.99	11.57	3.8	4.0
Null Hypothesis		rejected	rejected	accepted	accepted	accepted	accepted

**Fig. 3.** Automated terminal extraction.**Fig. 4.** Manual terminal extraction.

5 Stage-by-Stage Description of the Algorithmic Scheme

This section describes the results produced by applying the algorithmic scheme to initial data. Each scheme substep is provided with a brief description.

The steps concerning preprocessing and image analysis are described as follows: (1) the general characterization of the transformation or algorithm used; (2) mathematical content; and (3) the role of the given transformation in the solution to the problem under study.

The following conventional notation is used in the formulas for the transformations: \ominus is the erosion, \oplus is the dilatation, $\rho_I(J)$ is the reconstruction of the image I from the image J , and $*$ is a dual operator.

5.1 Preprocessing

All the substeps at stage 1 are intended to avoid oversegmentation when watershed transformation is applied to the morphological gradient image.

Substep 1.1 in the scheme is intended to eliminate narrow background peaks from the initial image. This step is essential for the reduction of background regions containing many local intensity minima, which are used as markers of objects at the next stage.

The transformation at stage 1.1 is as follows: erosion [6] with a flat structuring element B is applied to the initial image I ; then the resulting image is used as a marker in the reconstruction of the initial image:

$$I \circ_{\rho} B = \rho_I(I \ominus B) . \quad (1)$$

The structuring element for the erosion is a flat disk with a radius that is larger than the radius of a disk inscribed in any terminal and is smaller than the radius of a disk containing any terminal.

The main goal of substep 1.2 is to correct the complex heterogeneous background of the initial image. The inner structure of terminals remains the same under this transformation.

In the bot-hat transformation by dual reconstruction [6, 2] (stage 1.2), the initial image is subtracted from that obtained by closing the initial image by dual reconstruction:

$$BotHat_{\rho}^B(I) = \rho_I^*(I \oplus B) - I . \quad (2)$$

This transformation is used to eliminate the complex heterogeneous background from images of objects whose brightness values are less than the background brightness. The essence of the transformation is that, with a proper choice of the structuring element (such that each object is contained entirely in the structuring element), narrow areas of higher brightness can be marked without marking wide areas of higher brightness, which gives a good approximation of the background. The subtraction of the initial image from the "closed" one yields a more homogeneous background. The dual reconstruction is used to preserve the brightness values inside objects that are not completely smoothed by dilatation.

Substep 1.3 is used to smooth nonuniform regions in the interior of the terminals. This substep is essential for providing robust marking of the terminals. The transformation used at this stage is as follows: dilatation [6] with a flat structuring element B is applied to the initial image I ; then the resulting image is used as a marker in the dual reconstruction of the initial image:

$$I \bullet_{\rho} B = \rho_I^*(I \oplus B) . \quad (3)$$

In the general case, closing by dual reconstruction [6, 2] is used to eliminate narrow areas of higher brightness while preserving the average grayscale background and wide areas of changing brightness. The concepts of narrowness and wideness depend on B . In contrast to the usual closing procedure, the erosion of the dilated image with the same structuring element only partially reconstructs the brightness values of areas that were not completely smoothed by dilatation.

The aim of substep 1.4 is to eliminate out-of-focus objects. H-dome elimination corresponds to the removal of out-of-focus objects.

Reconstruction [9, 6, 2] is a highly effective method for extracting regional maxima and minima [9] from grayscale images. Moreover, this technique can be extended to structures known as h -maxima and h -minima.

According to [9], the binary image (mask) $M(I)$ of the regional maxima of I is given by the formula

$$M(I) = I - \rho_I(I - 1) . \quad (4)$$

The h -maximum transformation $D_h(I)$ is defined as:

$$D_h(I) = I - \rho_I(I - h) . \quad (5)$$

In contrast to the top-hat transformation, the h -maximum transformation extracts light structures without taking into account their shapes and sizes. The only parameter h is related to the height of these structures.

A technique for h -parameter estimation was offered for automation of the segmentation procedure. It proceeds on the idea of the selected regional minima clustering into two groups and setting h to be equal to a threshold value.

5.2 Image Analysis

A substantial drawback of the watershed algorithm is oversegmentation, which is caused by the noise or other local irregularities in the gradient image. A highly effective way of reducing oversegmentation is based on the idea of markers [8]. We distinguish between objects (inner markers) and background (outer) markers. Markers are used for the gradient image transformation. When the watershed segmentation algorithm is applied to the modified gradient, only marked objects are selected.

Object markers are extracted as regional minima of the image obtained at the previous stage. Background markers are estimated from the image obtained by applying the distance transformation [2] to the binary image of object markers. In this transformation, each image point is assigned a value equal to the distance to the nearest non-background pixel. Next, the watershed segmentation procedure [2, 8] is applied to the resulting image. As a result, the watershed lines are associated with pixels lying at the maximum distance from the nearest inner markers.

The morphological gradient is the image subject to dilatation minus the same image subject to erosion:

$$G(p, q) = (I \oplus B)(p, q) - (I \ominus B)(p, q) . \quad (6)$$

At stage 2.2, the gradient image G is transformed by grayscale reconstruction into an image G' [9] such that the local minima of G' coincide with the markers, while the line watershed lines separating the markers are fixed.

Let G be the gradient image, M — be the binary image of markers, and m be the maximum brightness value of G then

$$G' = \rho_{\min(G+1, (m+1)M)}^*((m+1)M) . \quad (7)$$

In this transformation, the pixels marked as markers are assigned a value of 0, while the unmarked areas are filled.

5.3 Construction of Object Representations

The following features (Table 2) were used to describe terminals at stage 3.1 of the scheme:

Table 2. Features.

Morphometric	Densitometric	Textural
geometric features:	intensity features of different image zones:	intensity features of different image zones:
<ul style="list-style-type: none"> – perimeter, – area, – elongation; 	<ul style="list-style-type: none"> – optical density, – standard deviation, – excess; 	<ul style="list-style-type: none"> – homogeneity, – smoothness, – entropy;
invariant-moments:	invariant-moments:	Fourier energy spectrum features:
<ul style="list-style-type: none"> – first two moments; 	<ul style="list-style-type: none"> – first seven moments; 	<ul style="list-style-type: none"> – mean, – peak, – dispersion, – difference between mean and maximum values along radius, depending on angle;

At stage 3.2 a successive algorithm for feature selection was used to find the most discriminate features when the terminals are classified into experiment and control groups. Fisher discriminant analysis was used for classification. The following features were selected as the most informative: the optical density, elongation, entropy, the first and third intensity distribution invariant-moments, and the dispersion of the Fourier energy spectrum along the circle centered at the centre of gravity of a terminal. Due to the feature selection algorithm, the accuracy of classification was increased from 67% to 74%.

5.4 Classification

At this stage of the algorithmic scheme, the terminals were clustered into 2 and 5 well-separated groups by applying different modern clustering techniques. Each cluster was provided with a statistical description including the probabilities of clustered objects belonging to a specified group (according to the animal type, brain area, section depth).

5.5 Software Implementation

The method developed has been implemented in a software code and is used for automated feeding and study of PD models.

The software implementation of the algorithmic scheme has the following features: (1) automated segmentation of brain section images of terminals; (2) the extraction of morphometric features (perimeter, area, elongation); (3) the extraction of densitometric features (statistics of the optical density distribution); (4) a database for storing the results; (5) processing of images separated into specified groups; (6) automated grouping of initial images by different methods (all pairs of experimental animals, various brain

domains (dorsal and ventral), in the direction of sections); (7) the calculation of statistics (expectation, standard deviation, standard error) and testing hypotheses concerning the distribution differences between the experimental and control groups for a given set of images (Student's t-test: statistics, significance level, accepted hypothesis).

The experimental results have shown that (1) the number of terminals of DA-ergic axons in the experimental group decreases considerably as compared with that in the control group; (2) the functional activity of DA-ergic terminals changes after neurotoxin administration. The results are an important step in the estimation of the nigrostriatal system in the PD brain. They can be used in the study of brain compensatory mechanisms with the aim of controlling them in the future.

In addition to the problem under study, the method was used to analyze arcuate nucleus sections with DA-ergic terminals in mice after neurotoxin administration. The number of processed images was about 2000. As a result, data were obtained concerning the effect of neurotoxin administration on the tuberoinfundibular system in mice, which is the first attempt to estimate the functional condition of this system.

6 Conclusions

We proposed a new method and a standardized algorithmic scheme for reducing brain section images to a form appropriate for recognition. The scheme was used as a basis for a software implementation of the method developed. It is currently being employed to estimate the degeneration and changes in the functional condition of DA-ergic axons in the striatum at different early stages of PD. The results are an important step in the estimation of the condition of the dopaminergic nigrostriatal system research at developing PD. The same methods can also be applied to similar task. In particular, they can be used to estimate the degeneration of DA-ergic neurons in the substantia nigra after neurotoxin administration and to estimate the functional conditions of dopaminergic neurons remaining after neurotoxin administration.

Experimental applications of the developed technique confirmed its high efficiency and suitability for the automated processing and analysis of brain section images (a 200 times increase in productivity and a 10 times decrease in the amount of animals and expendables).

References

1. Albin, R.L., Young, A.B., Penney, J.B.: The functional anatomy of basal ganglia disorders. *Trends Neurosci* 12, 366–75 (1989)
2. Gonsales, R.C., Woods, R.E.: *Digital Image Processing*. Pearson Education, Inc, 2 edn. (2002), publishing as Prentice Hall
3. Gurevich, I., Harazishvili, D., Jernova, I., et al.: Information technology for the morphological analysis of the lymphoid cell nuclei. In: *The 13th Scandinavian Conference on Image Analysis*. LNCS, vol. 2749, pp. 541–548 (2003)
4. Gurevich, I.B., Yashina, V.V., Koryabkina, I.V., Niemann, H., Salvetti, O.: Descriptive approach to medical image mining: An algorithmic scheme for analysis of cytological specimens. *Pattern Recognition and Image Analysis: Advances in Mathematical Theory and Applications* 18(4), 542–562 (2008)

5. Ogawa, N., Mizukawa, K., Hirose, Y., Kajita, S., Ohara, S., Watanabe, Y.: Mptp-induced parkinsonian model in mice: biochemistry, pharmacology and behavior. *Eur Neurol* 26 Suppl 1, 16–23 (1987)
6. Soille, P.: *Morphological Image Analysis: Principles and Applications*. Springer, Berlin (2004)
7. Tipton, K.F., Singer, T.P.: Advances in our understanding of the mechanisms of the neurotoxicity of mptp and related compounds. *J Neurochem* 61, 1191–1206 (1993)
8. Vincent, L., Soille, P.: Watersheds in digital spaces: an efficient algorithm based on immersion simulations. *IEEE Trans. Pattern Anal. Machine Intell.* 6(12), 583–598 (June 1991)
9. Vincent, L.: Morphological grayscale reconstruction in image analysis: Applications and efficient algorithms. *IEEE Transactions on Image Processing* 2, 176–201 (1993)

